ACS OMEGA

Open Access

http://pubs.acs.org/journal/acsodf

Article

Study on Reaction Mechanism and Process Safety for Epoxidation

Chunsheng Cheng,* Zhenyun Wei, Xu Ming, Jie Hu, and Rong Kong

Cite This: *ACS Omega* 2023, 8, 47254−47261

Read Online

ACCESS | Metrics & More | Article Recommendations | Supporting Information

ABSTRACT: The reaction mechanism and process safety for epoxidation were investigated in this study. 1-(2-Chlorophenyl)-2-(4-fluorophenyl)-3-(1,2,4-triazole) propene (triazolene), a typical representative of high steric olefinic compounds, was chosen as the raw material. In addition, hydrogen peroxide was chosen as the oxygen source in the reaction. Online Raman spectroscopy combined with high-performance liquid chromatography (HPLC) was used for the process monitoring analysis. The results of this study indicated that the epoxidation process is exothermic, and the apparent reaction heat was 1340.0 kJ·kg^{-1} (measured by the mass of triazolene). The heat conversion rate was 39.7% immediately after hydrogen peroxide dosing to a triazolene and maleic anhydride mixture solution in chloroform. This result indicated that a considerable amount of heat is accumulated during the epoxidation reaction, which leads to a potential high safety concern. The study of the reaction mechanism showed that maleic anhydride reacts with hydrogen peroxide quickly to form maleic acid peroxide, which is controlled by hydrogen peroxide feeding, and the formed maleic acid peroxide further reacts with triazolenes slowly, which is a kinetically controlled reaction. Decomposition kinetics studies revealed that the temperatures corresponding to the time of maximum reaction rate for 8 and 24 h are T_{D24} = 89.9 °C and T_{D8} = 104.1 °C, respectively.

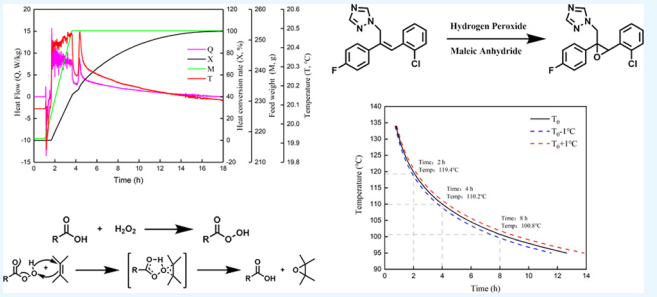

1. INTRODUCTION

Epoxidation of alkenes is a very important oxidation reaction,[1] which aims to form an epoxide compound by adding one atom of oxygen between the carbon atoms at both ends of the double bond of alkenes.[2] The Epoxide compound is one of the most valuable compounds in the pharmaceutical and spice industries.[3−5] In addition, it has an active ternary epoxy structure, which is prone to ring-opening reactions under various conditions, resulting in high-value-added chemical products and intermediates.[6,7] At present, the traditional epoxidation methods are mostly used in industry, the halogen alcohol method and peroxide acid method are mainly used to prepare epoxide compounds.[8] The halogen alcohol method[9] was widely used in the early industrial preparation of Epoxide, but its synthesis process was complicated, and the separation and treatment of byproducts were difficult and then caused serious environmental pollution. Now, this method has been phased out in industrial production. The peroxide acid method[10] is a relatively simple epoxidation method of olefins. Based on the different epoxidation methods, it can be classified into direct oxidation and indirect oxidation.[11] In direct oxidation, the olefins react directly with organic peroxy acids, such as performic acid, peracetic acid, and peroxy benzoic acid. In indirect oxidation, organic peroxy acid is generated during the process and immediately participates in epoxidation with olefins. Because of the high price of organic peroxy acid and the existence of instability, it is easy to decompose, inconvenient to store, and involves other security risks. The indirect oxidation method is thus typically used for epoxidation in industry.

A high concentration of hydrogen peroxide was commonly used as the oxidant in indirect epoxidation, and hydrogen peroxide is also unstable, heat, light, heavy metals, and other impurities will result in its decomposition, oxygen gas, and heat released.[12−14] Under the influence of reactant activity, hydrogen peroxide and peroxy acid accumulate at different degrees during the reaction and decompose rapidly when heated.[15] In addition, the epoxidation reaction itself is highly exothermic,[16,17] once the temperature is out of control, extremely easy to cause reaction accidents.[18−21] Therefore, the study on the safety of the indirect epoxidation process is helpful to avoid serious safety accidents in industrial processes and has important practical significance.

In this paper, the synthesis of epoxiconazole was chosen as a typical indirect epoxidation of highly hindered substituted olefins. Epoxiconazole is a famous broad-spectrum fungicide commonly used in agricultural production[22] and its effect inhibits synthesizing pathogenic ergosterol and hinders the pathogenic cell wall from forming.[23] It is an effective preventative measure against leaf spots, mildew, and spotting

Received: September 27, 2023
Revised: October 18, 2023
Accepted: November 16, 2023
Published: November 29, 2023

for bananas, green onions, garlic, celery, kidney beans, melons, asparagus, peanuts, sugar beets, and other crops.[24,25] The indirect epoxidation synthesis of fluconazole is carried out using triazolene as the raw material, using hydrogen peroxide and maleic anhydride to react to generate peroxy acid for epoxidation,[26] as shown in Scheme 1.

Scheme 1. Chemical Reaction Showing the Formation of Epoxiconazole

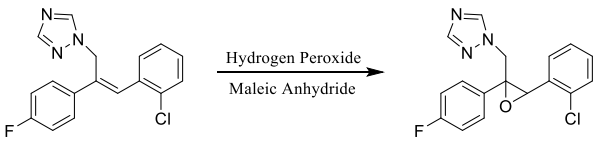

The safety of the indirect epoxidation process has not been reported. In view of the hazard of epoxidation, the process of synthesizing epoxiconazole was studied by online Raman combined with offline HPLC for the first time, clarifying the space-time rule and potential risk distribution of peroxide formation. Then the exothermic characteristics of the epoxidation process were studied by reaction calorimeter RC1, and the safety of the mixed system in different reaction stages was tested by TSU. Finally, the decomposition kinetics of the mixed system after the reaction was studied, and the relevant kinetic parameters were obtained. The change of reaction rate and conversion with time was simulated under adiabatic conditions. It provides the technical basis for final industrialization safety control.

2. EXPERIMENT

2.1. Reagents. Hydrogen peroxide (50%), maleic anhydride (≥99%), sodium bisulfate (≥99%), and chloroform (≥99%) were all purchased from China Pharmaceutical Group Co., Ltd. 1-(2-Chlorophenyl)-2-(4-fluorophenyl)-3-(1,2,4-triazole) propene (95%) was purchased from Shanghai Aladdin Biochemical Technology Co., Ltd. All reagents were used without further purification.

2.2. High-Performance Liquid Chromatography. High-performance liquid chromatography (Waters1525); Agilent SB-C18 (150 mm × 4.6 mm (i.d),5 μm). Mobile phase: acetonitrile/methanol/water (volume ratio: 40:20:40); column temperature: 30 °C; flow rate: 1.0 mL/min; detection wavelength: 230 nm.

2.3. Automatic Reaction Calorimeter. A reaction calorimeter (RC1e; Mettler Toledo, Zurich, Switzerland) was used to assess the exothermic conditions during the process. IControl software is used to analyze the test data processing, and can get the heat flow (Q), thermal conversion rate (X), heat transfer coefficient (U), adiabatic temperature rise (ΔT_{ad}), specific heat (C_p), and other thermodynamic information.

2.4. Thermal Screening Unit. A thermal Screening Unit (TSU; HEL, United Kingdom) was used to study the thermal decomposition characteristics of the reactants. The test ball is constructed using Hastelloy with a volume of 10 mL. The temperature range was from 30 to 300 °C. The operating pressure range is 0−100 bar, the heating rate is 5 K/min, and the loading volume is 1−3 g.

2.5. Online Raman Spectroscopy. An Online Raman spectrometer (ReactRaman 785; Mettler Toledo) was used to monitor the reaction process. By comparing the disappearance rate of the significant absorption peak of the reactant and the formation rate of the significant absorption peak of the product, the existence of active intermediates in the reaction process is judged.[27,28] The collection time of a single spectrogram is set as 15 s and the Raman exposure time as 1 s.

2.6. Differential Scanning Calorimetry. A differential scanning calorimetry (HP DSC1, Mettler Toledo) was used for thermal safety study of a milligram sample to obtain the thermal decomposition status of the sample to be tested. The samples were contained in a high-pressure gold-plated crucible with a volume of 30 μL. The sample mass was 3.0 ± 0.2 mg and the temperature range was 30−350 °C. The heating rates selected in these experiments were 3, 5, and 8 K/min.

2.7. Synthesis Method. Triazolene chloroform solution (wt 20%) (134 g, 0.0855 mol, 1.0 equiv) and maleic anhydride (83.8 g, 0.8551 mol, 10.0 equiv) were added to a 500 mL reactor, and the mixture was cooled to 20 ± 1 °C after full dissolution. Sodium bisulfate (0.2 g, 0.0020 mol, 0.02 equiv) was added, and wt 50% hydrogen peroxide (35.0 g, 0.5130 mol, 6.0 equiv) was dropwise added in 2.5 h, and the temperature was kept at 20 ± 1 °C for 16−20 h after dropwise addition finished. Sampling and analysis to triazolene were less than 10% as the reaction end point. The NMR characterization[29] of the product is shown in Figures S1 and S2.

3. RESULTS AND DISCUSSION

3.1. Reaction Mechanism. The C═C double bond changes from a one-dimensional linear moiety to a C−O−C two-dimensional plane in epoxidation. First, the acid anhydride reacts with hydrogen peroxide to form peroxy acid, and then, the peroxy acid reacts with alkene.[30] The epoxide is obtained through a transition state. The reaction mechanism is shown in Scheme 2, which was further verified by online Raman spectroscopy combined with HPLC.

Scheme 2. Epoxidation Reaction Mechanism

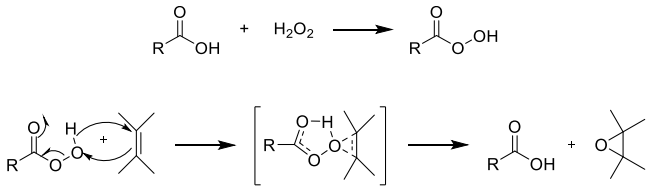

3.1.1. Characteristic Peak Identification. Online Raman spectroscopy was used for analyzing chloroform, maleic anhydride, and hydrogen peroxide. The results of the Raman spectral analysis of each starting material are shown in Figure 1.

Spectral analysis revealed that the primary characteristic absorption peaks are at 260 cm^{-1} (Cl−C−Cl degeneracy bend), 366 cm^{-1} (Cl−C−Cl symmetrical bend), and 667 cm^{-1} (C−Cl symmetrical stretch) for chloroform;[31,32] 635 cm^{-1} (ring deformation), 869 cm^{-1} (C−C stretch), 1065 cm^{-1} (C−O stretch), 1592 cm^{-1} (C═C stretch), and 1849 cm^{-1} (C═O stretch) for maleic anhydride;[33] and 881 cm^{-1} (O−O stretch) for hydrogen peroxide.[34]

3.1.2. Process Monitoring. Combined online Raman spectroscopy and HPLC analysis were adopted to monitor the reaction process in this study. The peaks at 1849, 881, and 1149 cm^{-1} were selected as the characteristic absorption peaks of maleic anhydride, hydrogen peroxide, and maleic acid peroxide,[35] respectively. The concentration changes of the triazolene starting material and epoxiconazole during the

https://doi.org/10.1021/acsomega.3c07461
ACS Omega 2023, 8, 47254−47261

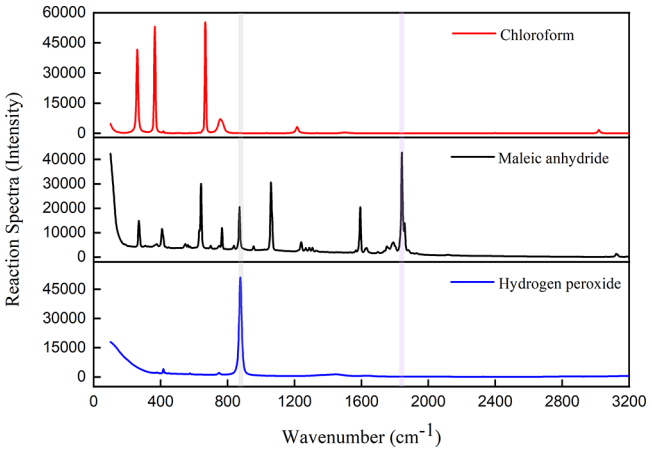

Figure 1. Raman spectra of the main raw materials.

reaction were analyzed using HPLC. The relative concentration changes of each component in the reaction are shown in Figure 2.

The results showed that the characteristic absorption peak of hydrogen peroxide at 881 cm^{-1} increased rapidly with hydrogen peroxide feeding, which is marked with a blue line (Figure 2). Conversely, the characteristic absorption peak of maleic anhydride at 1849 cm^{-1} showed a rapid decrease (black line). Furthermore, the characteristic absorption peak of maleic acid peroxide at 1149 cm^{-1} increased rapidly (red line). In the hydrogen peroxide feeding stage, maleic anhydride promptly reacts with hydrogen peroxide to generate maleic acid peroxide, which is a feeding control reaction. HPLC analysis showed that the conversion rate of triazolene was low, as indicated by the green line, and epoxiconazole was produced less, as indicated by the pink line in the hydrogen peroxide feeding stage. After the completion of hydrogen peroxide feeding, the conversion rate of triazolene and the generation of epoxiconazole gradually increased. Some solid epoxiconazoles were generated in the reaction system. The conversion of triazolene to epoxiconazole was related to the concentration of maleic acid peroxide in the system, and the reaction was kinetically controlled.

3.2. Exothermic Properties of the Epoxidation Reaction. The exothermic characteristics of the epoxidation process are shown in Figures 3 and 4.

Triazolene and maleic anhydride were added to chloroform to form a suspension solution, and 50% hydrogen peroxide was added dropwise when the temperature was decreased to 20.0 °C ± 1 °C. When hydrogen peroxide was added, the solid in the suspension solution gradually dissolved, and a chemical reaction occurred. The reaction was initially endothermic, with a maximum endothermic rate of 13.5 $W{\cdot}kg^{-1}$. After 30 min of hydrogen peroxide feeding, the apparent reaction became exothermic, gradually reaching the maximum heat release rate of 15.7 $W{\cdot}kg^{-1}$. The solid material precipitated out of the reaction medium as the feeding progressed; the heat release rate gradually decreased, and the average heat release rate throughout the dripping of hydrogen peroxide was 6.2 $W{\cdot}kg^{-1}$. After hydrogen peroxide feeding, the reaction heat conversion rate was 39.7%; this indicates considerable heat accumulation during the reaction process. After 30 min, the reaction heat release rate suddenly increased with accelerated solid precipitation. After maintaining for 11 h, the system exhibited no notable thermal effect.

The results of the current study reveal that the specific heat capacity for the reactant liquid is 3.13 $kJ{\cdot}kg^{-1}{\cdot}K^{-1}$, the epoxidation reaction process was overall exothermic, and the total apparent heat release was 268.0 $kJ{\cdot}kg^{-1}$ (based on the mass of the triazolene chloroform solution). The adiabatic temperature rise was 45.6 K, reaction heat accumulation was 60.3%, and the maximum temperature of the synthesis reaction (MTSR) was 47.5 °C when the cooling system failed.

3.3. Process Safety. *3.3.1. Thermal Stability Study during the Reaction.* The stability and safety of the epoxidation reaction system were studied in different stages by a thermal stability test. We collected four samples denoted as *a*, *b*, *c*, and *d*. Sample *a* is collected at the end of the hydrogen peroxide feeding; *b* is the reaction mixture kept warm for 3 h; *c* is the reaction mixture kept warm for 6 h; and *d* is the reaction mixture collected at the end of the reaction. The results are shown in Figure 5.

The results show that the samples at each stage of the reaction are thermally unstable, and the temperature and pressure showed a sharp rise with more heat release at 35−50 °C for each sample. With the extension of the holding time, the maximum temperature and pressure rise rate gradually decreased (Figure 6). At the end of hydrogen peroxide feeding, the maximum temperature rise rate of sample a was 31 times more, and maximum pressure rise rate was 41 times more than that of

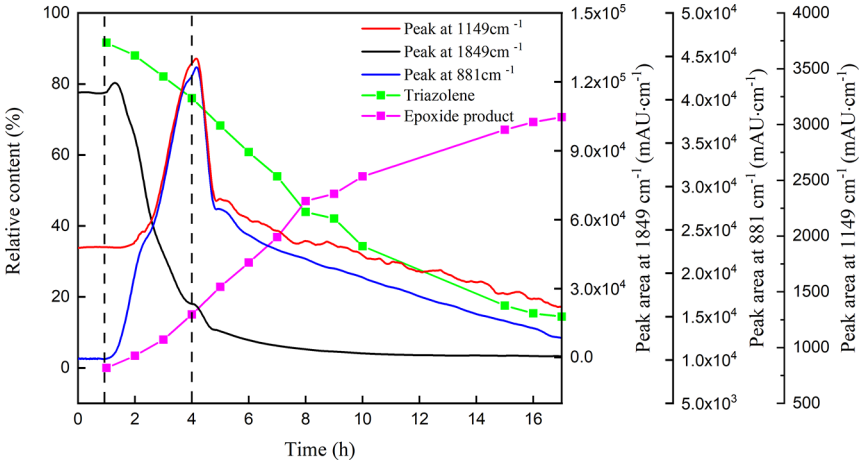

Figure 2. Reaction trend of each component. (Hydrogen peroxide is added in the dashed interval.)

https://doi.org/10.1021/acsomega.3c07461
ACS Omega 2023, 8, 47254−47261

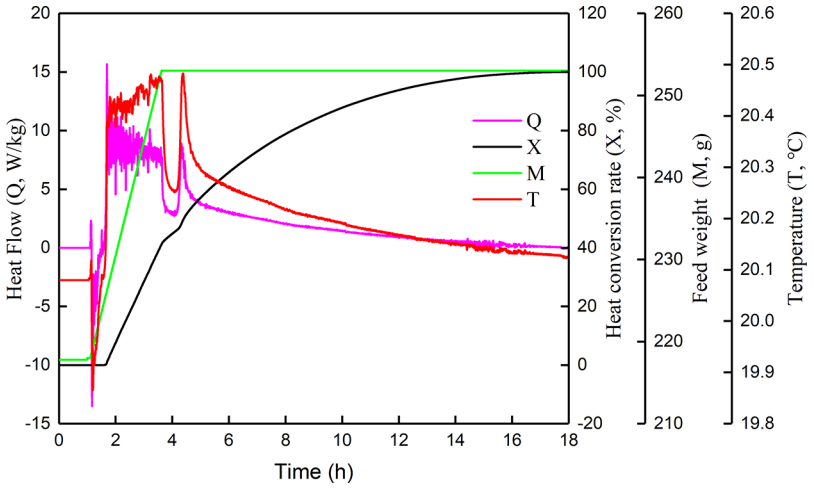

Figure 3. Reaction heat flow rate curve.

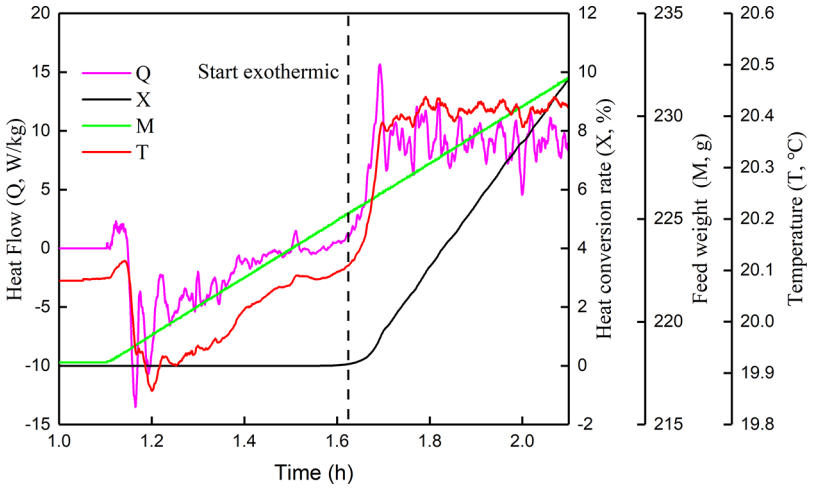

Figure 4. Reaction heat flow rate curve in the early stage.

sample *d*. A large amount of the maleic acid peroxide intermediate was generated in the reaction system during hydrogen peroxide feeding, resulting in the highest risk of decomposition. Therefore, risk control measures such as emergency quenching and overpressure relief must be established to avoid explosions in upscale tests and industrial applications of the epoxidation reaction.

3.3.2. Kinetics of Thermal Decomposition. In this study, considering the influence of the two important factors, conversion rate α and temperature T,[36] and that these two parameters are independent of one another, the reaction rate equation can be expressed as

$$d\alpha/dt = f(\alpha)\cdot k(T)$$

where α is the conversion rate, t is the reaction time, and $f(\alpha)$ is the reaction mechanism function.

The rate constant k is closely related to temperature T. Applying the Arrhenius equation, the following equation is obtained:

$$d\alpha/dt = f(\alpha)\cdot A(\alpha)\cdot \exp(-E/RT)$$

where T is the temperature in Kelvin, t is the time in seconds, E is activation energy kJ·mol^{-1}, $A(\alpha)$ is the pre-exponential factor with the unit s^{-1}, and R is the universal gas constant with the unit kJ·mol^{-1}·K^{-1}.

According to the reaction rate equation, the activation energy for the decomposition reaction is closely related to the reaction rate, conversion rate, and temperature. A differential scanning calorimeter was used to determine the variation trend of the solid−liquid self-decomposition reaction rate after the epoxidation reaction using different scanning rates, as shown in Figure 7.

The results indicate that the increased temperature rate was reduced by 2.7 times, the initial decomposition temperature was decreased by 19.3 °C, and the maximum self-decomposition rate was reduced by 2.5 times. Because of this, a higher rate of temperature increase indicates a higher initial detected decomposition temperature. Using Friedman's equal conversion rate differential method,[37] AKTS (Advanced Kinetics and Technology Solutions) software obtained the activation energy for the decomposition reaction. Figure 8 shows that the activation energy for the self-decomposition reaction from the sample was 44−104 kJ/mol. The fluctuation range was extensive, indicating that the decomposition process of the sample was more complex.[38]

3.3.3. Decomposition Reaction Safety. Using the thermokinetic results, the decomposition thermokinetics for the time taken to the maximum reaction rate under adiabatic conditions

https://doi.org/10.1021/acsomega.3c07461
ACS Omega 2023, 8, 47254−47261

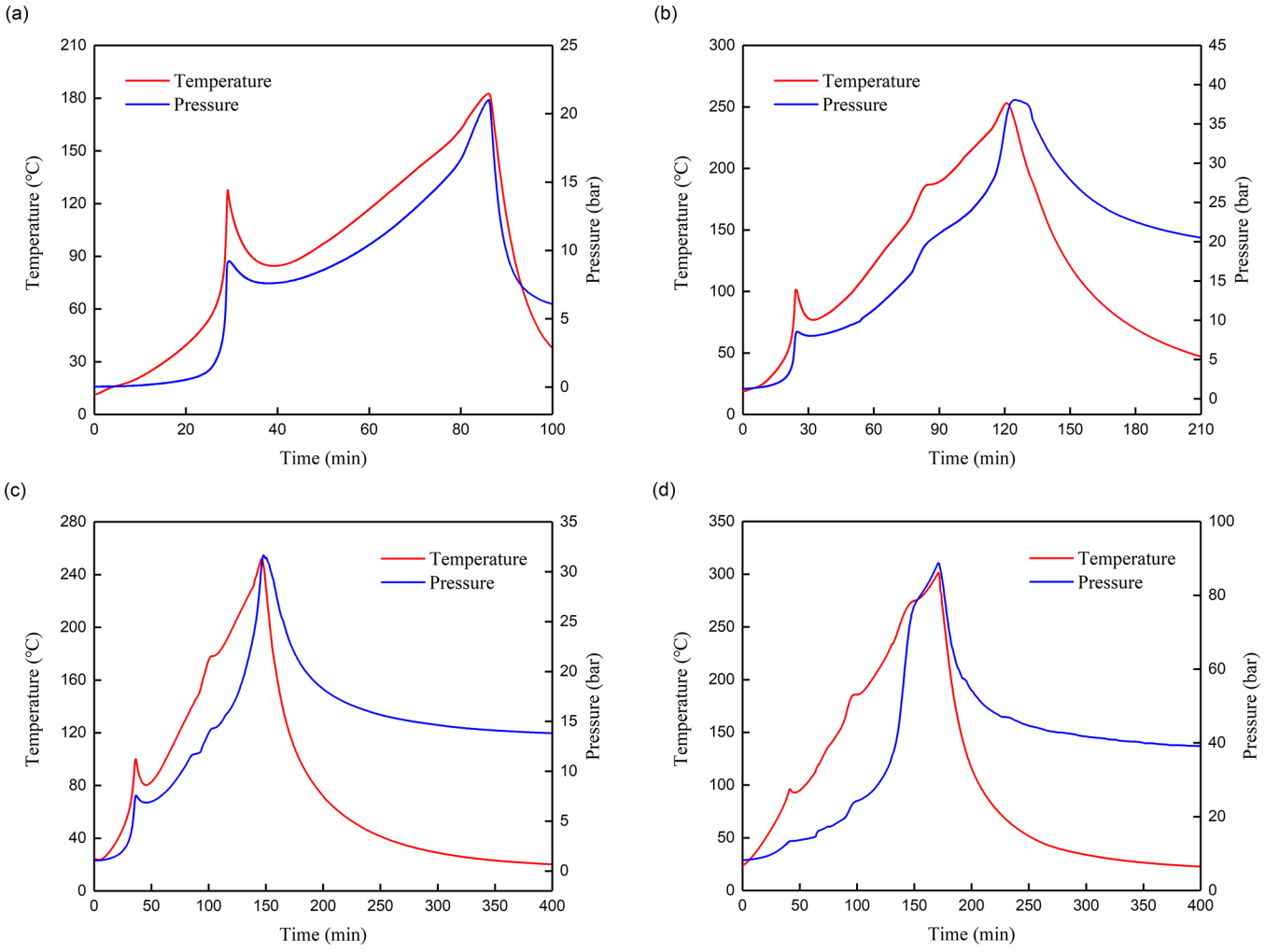

Figure 5. Time−temperature−pressure curve for the TSU calorimetric test. (a) End of the hydrogen peroxide feeding; (b) reaction mixture kept warm for 3 h; (c) reaction mixture kept warm for 6 h; and (d) reaction mixture collected at the end of the reaction.

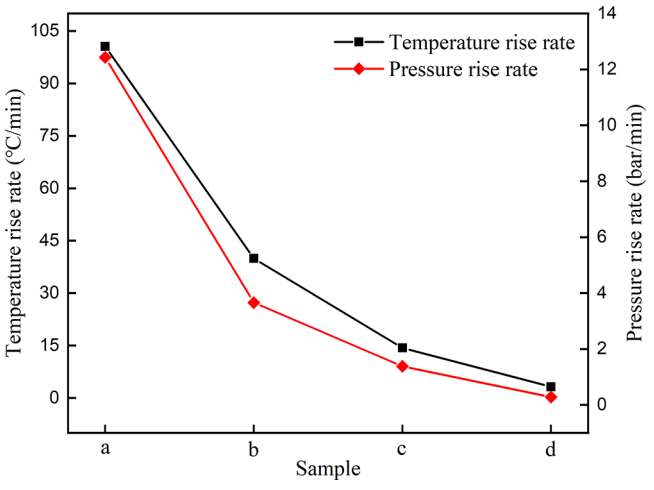

Figure 6. Relationship between temperature and pressure rise rate in each stage of epoxidation.

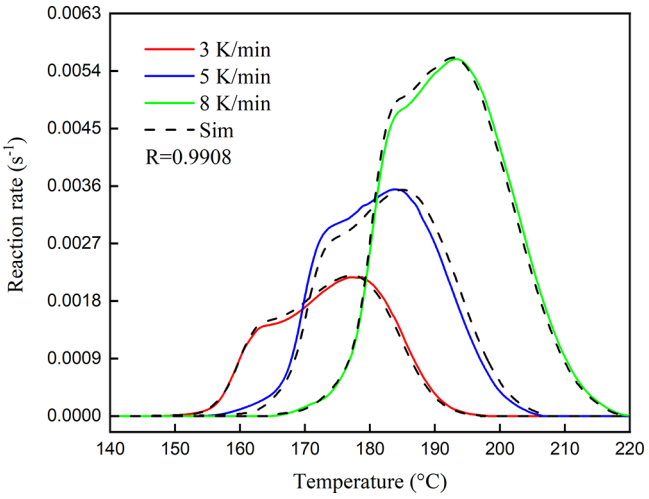

Figure 7. Variation trend of the self-decomposition rate.

(TMRad)[39] of the material solution after the epoxiconazole synthesis reaction were studied and analyzed. The results of the study are shown in Figure 9. Under adiabatic conditions, T_{D2} is the temperature at which the time to the maximum reaction rate for thermal decomposition is 2 h. Here, T_{D2} was 119.4 °C, while that at 4 h (T_{D4}) was 110.2 °C, that at 8 h (T_{D8}) was 100.8 °C, that at 24 h (T_{D24}) was 87.2 °C, and that at 168 h (T_{D168}) was 65.9. (the specific heat capacity for the sample was 3.13 kJ·kg^{-1}·K^{-1}, and the system Phi was 1.05).

https://doi.org/10.1021/acsomega.3c07461
ACS Omega 2023, 8, 47254−47261

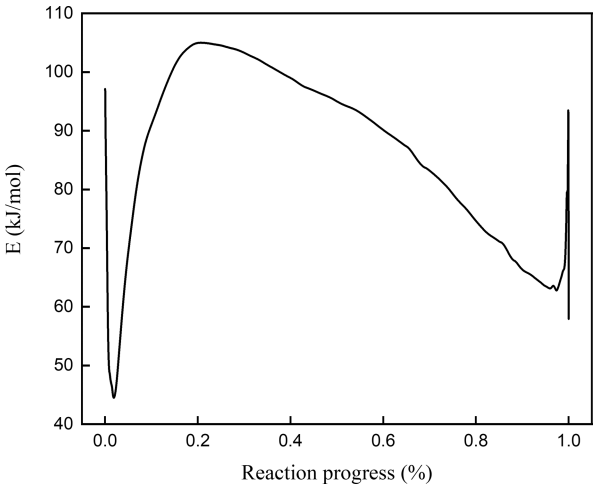

Figure 8. Activation energy of the self-decomposition reaction of the feed liquid after epoxidation.

T_{D8} and T_{D24} are the temperatures at which the time to the maximum reaction rate for material decomposition are 8 and 24 h under adiabatic conditions, which is critical for risk control in emergencies.[40] Considering the relationship between time, temperature, and conversion rate for the decomposition reaction, the results for the decomposition mechanics study for T_{D8} and T_{D24} are shown in Figures 10 and 11, respectively.

Under adiabatic conditions, when the sample was at 100.8 °C (T_{D8}), the initial decomposition reaction rate, decomposition reaction conversion rate, and sample temperature slowly increased. At 4.4 h, the decomposition reaction conversion rate increased to 16.1% and the decomposition reaction rate significantly increased. The decomposition reaction rate reached its maximum at 8 h, and the decomposition reaction conversion rate increased to 83.8%. At 8.8 h, all of the materials were decomposed.

Under adiabatic conditions, when the sample was at 87.2 °C (T_{D24}), the initial decomposition reaction rate, decomposition reaction conversion rate, and sample temperature slowly increased. At 12 h, the decomposition reaction conversion rate increased to 13.9%, and the decomposition reaction rate

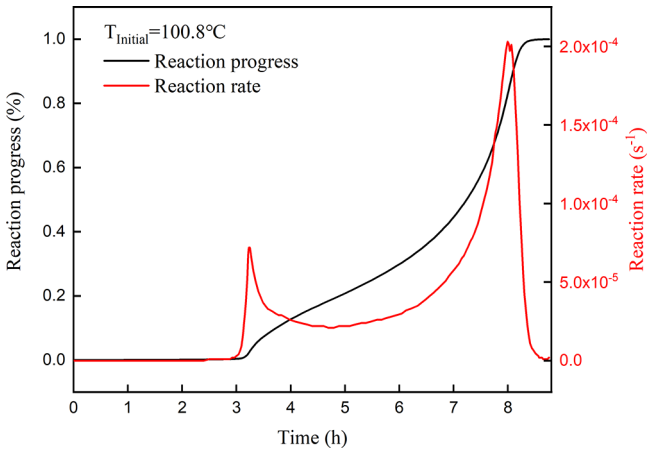

Figure 10. Trend of self-decomposition reaction at T_{D8} = 100.8 °C.

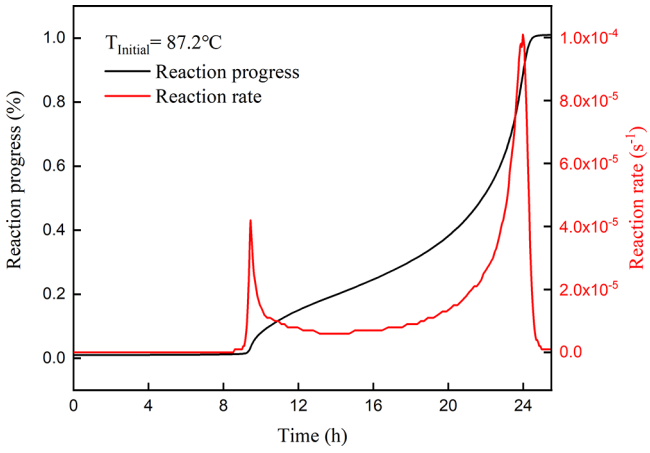

Figure 11. Trend of self-decomposition reaction at T_{D24} = 87.2 °C.

significantly increased. The decomposition reaction rate reached its maximum at 24 h, and the decomposition reaction conversion rate increased to 88.5%. At 25.4 h, all of the materials were decomposed.

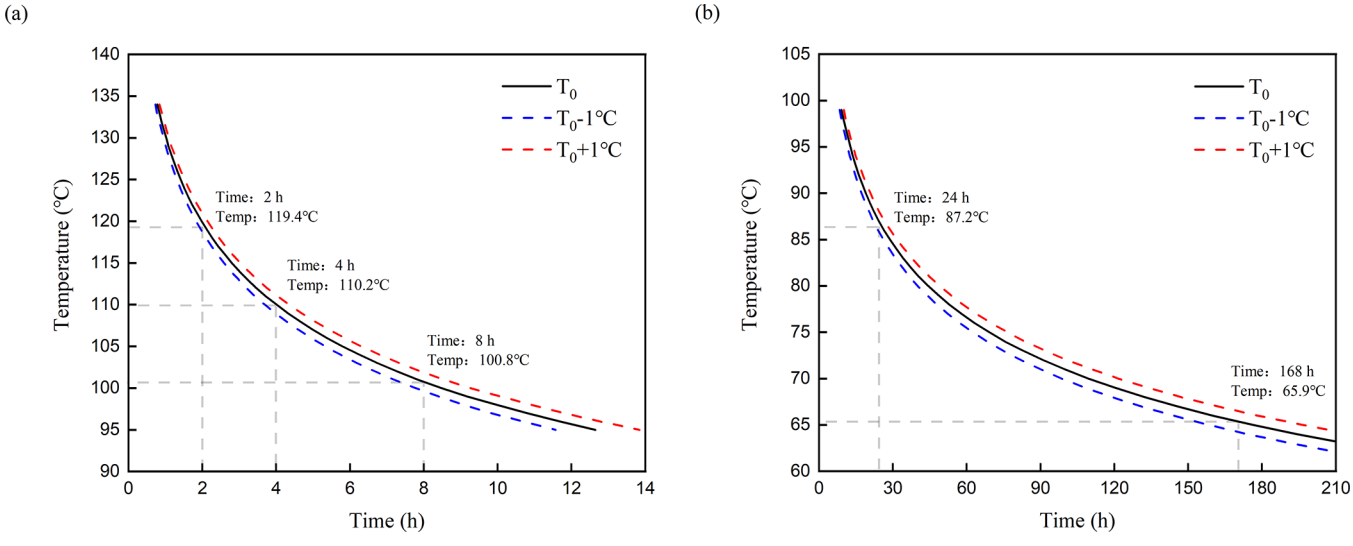

Figure 9. TMR_{ad} curve of the self-decomposition reaction of epoxidation. (a) 0−14 h; (b) 0−210 h.

https://doi.org/10.1021/acsomega.3c07461
ACS Omega 2023, 8, 47254−47261

4. CONCLUSIONS

The reaction mechanism and process safety for epoxidation of triazolenes and hydrogen peroxide as the oxygen source were studied herein, providing technical bases for their production, storage, and transportation. The results are summarized as follows:

(1) In the epoxidation of 1-(2-chlorophenyl)-2-(4-fluorophenyl)-3-(1,2,4-triazole) propene in the presence of maleic anhydride and with hydrogen peroxide as the oxygen source, maleic acid peroxide is produced first, and then, maleic acid peroxide reacts with triazolene to form the epoxiconazole. The former reaction is fast and is controlled by hydrogen peroxide feeding, while the latter is slow and is controlled by kinetics.

(2) The epoxidation process is complicated, involving solid maleic anhydride dissolution and epoxiconazole precipitation. The epoxidation process is exothermic, and the apparent reaction heat was 1340.0 kJ·kg^{-1}, the adiabatic temperature rise was 45.60 K, and the maximum temperature of the synthesis reaction (MTSR) was 47.5 °C when the reaction runaway occurred.

(3) The reaction runaway occurred at 35−50 °C at different stages along the complete process with a significant release of heat and gas, thereby raising serious safety concerns. At the end of hydrogen peroxide feeding, the temperature and pressure increase rates of decomposition are at their maximum values. The decomposition kinetics study showed that the temperatures corresponding to the time of maximum reaction rate are 89.9 °C (T_{D24}) and 104.1 °C (T_{D8}). The maximum temperature of the epoxidation reaction process was 47.5 °C when the reaction runaway occurred, which exceeds the temperature at which the mixture decomposes violently at different stages of the reaction, thus posing a potential safety hazard.

In the process of epoxidation reaction scale up and industrialization, control measures for emergency quenching and overpressure explosion relief should be established, and control measures should be started in a timely manner after the thermal runaway of the reaction system to avoid the violent decomposition of the materials leading to an accident.

■ ASSOCIATED CONTENT

Supporting Information

The Supporting Information is available free of charge at https://pubs.acs.org/doi/10.1021/acsomega.3c07461.

NMR characterizations of triazolene and epoxiconazole (PDF)

■ AUTHOR INFORMATION

Corresponding Author

Chunsheng Cheng − *Chemical Industry Safety Technology & Engineering Center, Shenyang Research Institute of Chemical Industry, Shenyang 110021 Liaoning, China*; orcid.org/0000-0001-7185-7560; Email: chengchunsheng@sinochem.com

Authors

Zhenyun Wei − *Chemical Industry Safety Technology & Engineering Center, Shenyang Research Institute of Chemical Industry, Shenyang 110021 Liaoning, China*

Xu Ming − *Chemical Industry Safety Technology & Engineering Center, Shenyang Research Institute of Chemical Industry, Shenyang 110021 Liaoning, China*

Jie Hu − *Chemical Industry Safety Technology & Engineering Center, Shenyang Research Institute of Chemical Industry, Shenyang 110021 Liaoning, China*

Rong Kong − *Chemical Industry Safety Technology & Engineering Center, Shenyang Research Institute of Chemical Industry, Shenyang 110021 Liaoning, China*

Complete contact information is available at: https://pubs.acs.org/10.1021/acsomega.3c07461

Author Contributions

Conceptualization was contributed by C.C. and Z.W.; methodology was contributed by X.M. and R.K.; resources were contributed by C.C.; writing (original draft preparation) was contributed by J.H.; writing—review and editing—was contributed by C.C. and Z.W.

Notes

The authors declare no competing financial interest.

■ ACKNOWLEDGMENTS

We gratefully acknowledge the financial support provided by the National Key Research and Development Program of 14th Five-Year Plan, China (Grant No. 2021YFC3001101).

■ ABBREVIATIONS

A	Pre-exponential factor of Arrhenius equation, s^{1}
Q	Heat flow, kJ
X	Thermal conversion rate, %
U	Heat transfer coefficient, W m^{-2}
ΔT_{ad}	Adiabatic temperature rise, °C
C_p	Specific heat capacity, kJ kg^{-1} K^{-1}
R	Gas constant, 8.314 J mol^{-1} K^{-1}
E	Apparent activation energy, kJ mol^{-1}
m	Mass, g
MTSR	Maximum temperature of the runaway system, °C
T	Temperature, °C
TMR_{ad}	Time to maximum rate under adiabatic conditions, h
T_{D8}	Initial process temperature at which TMR_{ad} is 8 h, °C
T_{D24}	Initial process temperature at which TMR_{ad} is 24 h, °C
P	Pressure, bar
t	Reaction time, s
β	Heating rate, °C min^{-1}
α	Conversion rate, %
Phi	Correction factor, dimensionless

■ REFERENCES

(1) Sun, Z.; Fan, M.; Russell, C. K.et al. Chemical looping-based energy transformation via lattice oxygen modulated selective oxidation *Prog. Energy Combust. Sci.* **2023**, *96*, 101045, .

(2) Jun, W.; Min, Y.; Xiaoquan, Y. Progress in epoxidation of olefins. *J. Nanjing Xiaozhuang Coll.* **2019**, *35* (6), 31−44. CNKI:S UN: SFZK.0.2019−06−008

(3) Satam, V. S.; Pedada, S. R.; Kamaraj, P.; et al. Development of a Scalable Process for the Synthesis of DNDI-VL-2098: A Potential Preclinical Drug Candidate for the Treatment of Visceral Leishmaniasis. *Org. Process Res. Dev.* **2017**, *21* (1), 52−59.

(4) Huang, K.; Xiao, Y.; Dong, Y.; Xu, X.; Zhang, R.; Lin, L. Effects of uniconazole on the physiological characteristics and cadmium accumulation of Cyphomandra betacea seedlings. *Environ. Prog. Sustainable Energy* **2021**, *40* (4), 13614.

(5) Brancato, A.; Brocca, D.; Carrasco, Cabrera L Modification of the existing maximum residue level for epoxide product in beetroots. *EFSA J.* **2018**, *16* (10), 5419.
(6) Wu, Y.; Chen, Z.; Wang, Y. Kinetic Studies and Reaction Network in the Epoxidation of Styrene Catalyzed by the Temperature-Controlled Phase-Transfer Catalyst *Ind. Eng. Chem. Res.* **2022**, *61*, 10747, DOI: 10.1021/acs.iecr.2c01318.
(7) Salmi, T.; Russo, V.; Aguilera, A. F.; et al. A new perspective on vegetable oil epoxidation modeling: Reaction and mass transfer in a liquid−liquid−solid system. *AIChE J.* **2022**, *5*, 68.
(8) Hui, Chang Development of olefin epoxidation technology and its catalysts. *Technol. Econ. Petrochem. Ind.* **2015**, *6*, 5.
(9) Meng, J. *Study on epoxidation of olefins*; East China Normal University, 2009.
(10) Lane, B. S.; Burgess, K. Metal-Catalyzed Epoxidations of Alkenes with Hydrogen Peroxide. *Chem. Rev.* **2003**, *103*, 2457 DOI: 10.1021/cr020471z.
(11) Xiaoyue, Y.; Huanfeng, J. Epoxidation of olefin using hydrogen peroxide as oxygen source *Org. Chem.* **2007**.
(12) Jiang, W.; Ni, L.; Jiang, J.; Chen, Q.; Chen, Z.; Ye, S. Thermal hazard and reaction mechanism of the preparation of adipic acid through the oxidation with hydrogen peroxide. *AIChE J.* **2021**, *67* (1), 17089.
(13) Fei, M.; Ni, L.; Yan, T.; et al. Process safety evaluation and reaction mechanism of two step synthesis of tert-butyl hydrogen peroxide. *Journal of the Taiwan Institute of Chemical Engineers* **2023**, *145*, No. 104776.
(14) Gómez-García, M. A.; Dobrpsz-Gómez, I.; Ojeda Toro, J. CThermal safety assessment for catalytic decomposition of hydrogen peroxide by dynamic analysis. Transactions of The Institution of Chemical Engineers *Process Saf. Environ. Prot., Part B* **2017**, *109*, 46, DOI: 10.1016/j.psep.2017.03.025.
(15) Ryan, A. A.; Dempsey, S. D.; Smyth, M.; Fahey, K. et al. Continuous Flow Epoxidation of Alkenes Using a Homogeneous Manganese Catalyst with Peracetic Acid *Org. Process Res. Dev.* 2023, *27*, 262, DOI: 10.1021/acs.oprd.2c00222.
(16) Xiaoyue, Y.; Huanfeng, J. Epoxidation of olefin using hydrogen peroxide as oxygen source *Org. Chem.* **2007**.
(17) Oakley, L. H.; Casadio, F.; Shull, K. R. Theoretical Study of Epoxidation Reactions Relevant to Hydrocarbon Oxidation *Ind. Eng. Chem. Res.* 2017, *56*, 7454, DOI: 10.1021/acs.iecr.7b01443.
(18) Zhang, F. Study on the safety of epoxidation of olefin with hydrogen peroxide as oxygen source. *Qingdao Univ. Sci. Technol.* **2015**, DOI: 10.7666/d.Y2773901.
(19) Moreno, V. C.; Russo, V.; Tesser, R.; et al. Thermal risk in semi-batch reactors: The epoxidation of soybean oil. *Process Saf. Environ. Prot.* **2017**, *109*, 529.
(20) Leveneur, S.; Estel, L.; Crua, C. Thermal risk assessment of vegetable oil epoxidation *J. Therm. Anal. Calorim.* **2015**, *122*(2), 795, DOI: 10.1007/s10973-015-4793-8.
(21) Pérez-Sena, W. Y.; Salmi, T.; Estel, L.; Leveneur, S. Thermal risk assessment for the epoxidation of linseed oil by classical Prisleschajew epoxidation and by direct epoxidation by H2O2 on alumina. *J. Therm. Anal. Calorim.* **2020**, *140* (2), 673−684.
(22) Xin, L.; Qiuxu, Y.; Ping, Z. Market overview of flucyclozole fungicides. *Pesticide* **2010**, *11*, 2.
(23) Wang, J.; Zhao, L.; Liu, X.; He, Z. Stereoselective effects of chiral epoxide product on the metabolomic and lipidomic profiling of leek. *Food Chem.* **2023**, *405*, No. 134962.
(24) Liu, C.; Wang, B.; Diao, J.; Zjou, Z. Enantioselective toxicity and bioaccumulation of epoxide product enantiomers to the green alga Scenedesmus obliquus. *RSC Adv.* **2016**, *6* (64), 59842−59850.
(25) Gottardi, Michele; Birch, Michala Rosa; Dalhoff, Kristoffer; Cedergreen, Nina The effects of epoxide product and α-cypermethrin on Daphnia magna growth, reproduction, and offspring size. *Environ. Toxicol. Chem.* **2017**, *36* (8), 2155−2166.
(26) Caixin, J.; Zuwei, C.; Linrong, Y. *Review on synthesis of flucyclozole*; Zhejiang Chem. Ind., 2006.
(27) Chane, Y.; Min, S.; Park, E.; Lim, C.; Cheon, C.; Jeong, K.; Kwak, K.; Cho, M. Real-Time Reaction Monitoring with In Operando Flow NMR and FTIR Spectroscopy: Reaction Mechanism of Benzoxazole Synthesis. *Anal. Chem.* **2021**, *93*, 2106 DOI: 10.1021/acs.analchem.0c03852.
(28) Shi, M.; Wang, R.; Li, L.; Chen, N.; Xiao, P.; Yan, C.; Yan, X. Redox-Active Polymer Integrated with MXene for Ultra-Stable and Fast Aqueous Proton Storage. *Adv. Funct. Mater.* **2023**, *33* (1), No. 2209777.
(29) Zeng, Q.; Bie, B.; Guo, Q.; et al. Hyperpolarized Xe NMR signal advancement by metal-organic framework entrapment in aqueous solution. *Proc. Natl. Acad. Sci. U. S. A.* **2020**, *117* (30), 17558.
(30) Qiyi, X. *Basic Organic Chemistry*; Higher Education Press, 1983.
(31) Cavagnat, D.; Brotin, T.; Bruneel, J. L.; et al. Raman Microspectrometry as a New Approach to the Investigation of Molecular Recognition in Solids: ChloroformCryptophane Complexes. *J. Phys. Chem. B* **2004**, *108* (18), 5572.
(32) Shirota, H.; Kato, T. Intermolecular vibrational spectra of C3v CXY3Molecular Liquids, CHCl3, CHBr3, CFBr3, and CBrCl3. *J. Phys. Chem. A* **2011**, *115* (32), 8797−807.
(33) Dai, Y.; Wang, K.; Li, X.; et al. High-Pressure-Induced Planarity of the Molecular Arrangement in Maleic Anhydride. *J. Phys. Chem. C* **2016**, *120*, 18503 DOI: 10.1021/acs.jpcc.6b06351.
(34) Zhao, W. Measurement of Raman χ (3) and Theoretical Estimation of DOVE Four Wave Mixing of Hydrogen Peroxide. *J. Phys. Chem. A* **2011**, *115*, 6525.
(35) Wei, Z.; Hu, J.; Ming, X.; Cheng, C.; Li, S. Preparation and safety of peroxymaleic acid. *Pesticide* **2022**, *61* (7), 5.
(36) Niu, H.; Chen, S.; Jin, S.; Li, L.; Jing, B.; Jiang, Z.; Ji, J.; Shu, Q. Thermolysis, nonisothermal decomposition kinetics, calculated detonation velocity and safety assessment of dihydroxylammonium 5, 5-bistetrazole-1, 1-diolate. *J. Therm. Anal. Calorim.* **2016**, *126* (2), 473−480.
(37) Friedman, H. L. Kinetics of thermal degradation of char-forming plastics from thermogravimetry. Application to a phenolic plastic. *J. Polym. Sci. Polym. Sym.* **1964**, *6* (1), 183−195.
(38) Yao, H.; Jiang, J.; Li, B. Investigation of pyrolysis kinetics, mechanism and thermal stability of tert-butyl peroxy-2-ethyl hexanoate. *Process Saf. Environ.* **2022**, *160*, 734−748.
(39) Wang, Y. R.; Liu, J. P.; Chen, L. P. et al. Thermal decomposition characteristics and runaway boundary conditions of HATO at adiabatic and high pressure situations *Process Saf. Environ. Prot., Part B* **2022**, *167*, 601, DOI: 10.1016/j.psep.2022.09.045.
(40) Zhang, H.; Jiang, J.-C.; Ni, L.; Shu. C.Pyrolysis mechanism and thermal hazard essence investigation using thermal analysis coupled with quantum-chemical DFT simulation for 1-butyl-2,3-dimethylimidazolium nitrate. *J. Mol. Liq.* **2022**, *363*, No. 119850.

https://doi.org/10.1021/acsomega.3c07461
ACS Omega 2023, 8, 47254−47261